IEEE Access
Multidisciplinary | Rapid Review | Open Access Journal

Received 7 August 2023, accepted 16 August 2023, date of publication 21 August 2023, date of current version 29 August 2023.

Digital Object Identifier 10.1109/ACCESS.2023.3306782

RESEARCH ARTICLE

A Digital Twin Model for Automatic Width Control of Hot Rolling Mill

CHAOQUN SONG, XIAOHUI SHEN, AND JUNCHAO XIA
School of Metallurgical Engineering, Anhui University of Technology, Anhui 243032, China
Corresponding author: Xiaohui Shen (sxh@ahut.edu.cn)

ABSTRACT Considering the head and tail deformation phenomenon in the slab rolling process, this paper studies the online width adjustment control problem of the continuous casting slab based on the digital twin framework. First, the material mechanical properties, geometric model and boundary conditions of the continuous casting slab rolling are given to establish the deformation model of the continuous casting slab rolling process by using the rigid-viscoplastic finite element method. Second, the deformation model of the rolled piece is mainly reflected by shape parameters of the head and tail. The feature design of the head and tail shape is carried out based on the finite element simulation results, and multi-layer perceptron is used to extract features and realize the model regression for obtaining a digital twin model. Then, in view of the parameters of the continuous casting slab, the digital twin model is used to predict the loss-width curve at the head and tail of the slab online, and then the roll gap of the vertical roll mill is corrected synchronously to realize the width adjustment technology of the continuous casting slab and reduce production costs. Finally, taking the slab rolling process of a steel factory as an example, the accuracy and effectiveness of the proposed method are illustrated.

INDEX TERMS Continuous casting slab, digital twin, finite element, multi-layer perceptron.

I. INTRODUCTION

A. BACKGROUND

The hot rolling production is an essential procedure in the whole steel rolling process, and it is also the key to the cloud-edge-end efficient collaborative management and control system. The hot-rolling digital intelligent manufacturing system is of great significance to promote the construction of high-quality intelligent factories [1], [2], [3]. At present, the continuous casting slab is basically used as raw materials in the production of hot strip rolling. During the rolling process, the slab shape changes with the rolling mill works, especially the head and tail parts [4], [5]. In order to improve the production efficiency of the continuous casting machine, it is necessary to reduce the width specification of the continuous casting slab as much as possible. For satisfying the needs of producing slabs of different widths and ensure the normal production of strip steel with various width specifications, the width of the crystallizer should be adjusted according to the width of the slab. Furthermore, the online width adjustment technology of the continuous casting slab in the roughing rolling unit of the strip steel production line is realized [6], [7], and the technology can continuously cast slabs of different widths without stopping the machine, which saves a lot of manpower and material resources, and greatly improves the production rhythm and efficiency. Especially when realizing the production needs of hot delivery and continuous casting and rolling, this technology is particularly important [8].

The associate editor coordinating the review of this manuscript and approving it for publication was Su Yan.

B. RELATED WORK NOW

For the purpose of solving the problem of significant width variation of the slab head and tail caused by edging and horizontal rolling, the short stroke control (SSC) strategy [9], [10], [11] is adopted according to the width reduction deformation curve of the slab head and tail, and the technology has been widely used in actual production. Therefore, modeling of slab deformation curve becomes particularly important. S. Xiong et al. conducted physical simulation

experiments to observe and summarize the deformation laws of slabs and analyzed the influencing factors of deformation [12]. The calculation equation of shape parameters is proposed to set the form and control parameters of the short stroke curve. However, this method has disadvantages of ignoring many factors affecting deformation, long research and development time, and large funds. With the growth of computer technology and computational mechanics, the finite element (FE) method has gradually been diffusely used in the steel industry. The FE method analyzes the metal deformation process with fewer artificial assumptions, and describes the deformation process more realistically. Compared with the physical simulation experiment method, the FE method can obtain data that cannot be obtained or is difficult to obtain by the experimental method, and can save experimental costs.

According to the constitutive relationship of materials, the FE method can be divided into elastic-plastic FE method [13], rigid-plastic/rigid-viscoplastic FE method [14], hyperelastic FE method [15]. Compared with other FE methods, the rigid-plastic/rigid-viscoplastic FE method transforms the solution of plastic partial differential equations into the problem of finding functional extremum in the form of energy rate integration. Through FE discretization, it is further transformed into a nonlinear algebraic equation about the node velocity, and other parameters such as strain rate and stress are calculated according to the obtained node velocity. Due to the avoidance of geometric nonlinear problems, the incremental step size of the rigid-plastic/rigid-viscoplastic FE method is relatively large, and it has the advantages of no cumulative error in stress calculation and short calculation time. Although ignoring the elastic deformation of the material brings some errors, for metals deformed at high temperatures, the plastic strain is much greater than the elastic strain, and this error can be ignored. Joun et al. made tool velocity and material velocity field as unknown variables, and approximately predicted the deformation of material in ring rolling by an axisymmetric rigid–viscoplastic FE method [16]. Tan et al. developed a 3D thermo-mechanical coupled model of the milling process using the rigid-viscoplastic finite element theory [17]. Carvalho presented a phenomenological viscoelastic-viscoplastic model for accurately simulating the large strain constitutive response of polymeric materials [18]. Liang et al. proposed a new FE formulation to apply a viscoplastic medium [19]. The above literature shows that the rigid-viscoplastic FE method is suitable for the deformation model analysis of different materials.

The stress changes in the rolling system are complex, and the accuracy of the FE simulation and the deviation from the actual results need to be strictly controlled to satisfy the rolling area width adjustment accuracy. The digital twin (DT) technology that has emerged in recent years can solve this problem well since it enables real-time connectivity between the physical and virtual worlds [20], [21], [22], [23]. More specifically, the DT model can simulate and replicate the real-time behavior of physical systems operating under life-cycle conditions. The construction process of the DT model includes geometric model construction, mechanism model construction, data model construction, data transmission and other parts [24], [25]. In practical engineering applications, these factors will affect the accuracy and efficiency of DTs. Establishing a model based on data is the most critical link in the process of a DT model, which affects the reliability and efficiency of the output. Combining physical models with dynamic data models is a logical solution to improve the efficiency of DTs. Li et al. established the fault progressive mechanism of the bearing in the whole life based on the measured signals, and obtained the DT model of the life-cycle rolling bearing with multi-scale fault in virtual space [26]. Xiang et al. designed an end-face defect control framework based on DT with cloud-edge collaboration for recognizing defect [27]. Lippi et al. presented a novel hierarchical architecture that utilizes the DT to build logical abstractions of the overall system and to learn causal models of the environment directly from data [28]. At present, the research of DT is mainly focused on the fault detection in the production process, and it has not been used to describe the deformation of the slab in the rolling process.

This paper mainly studies the problem of online width adjustment control in continuous casting slab rolling process. The main contributions are as follows:

- Given the material mechanical properties, geometric model and boundary conditions of the continuous casting slab, the deformation model of the rolling process is established by using the rigid-viscoplastic FE method.
- The FE simulation results are preprocessed, the feature parameters of the head and tail shape are determined, then multi-layer perceptron (MPL) is used to realize feature extraction and establish a DT model.
- In view of the DT model, the loss-width curve at the slab shape of the head and tail is predicted online, and then the roll gap of the vertical roller mill is corrected synchronously to realize the width adjustment and rolling of the continuous casting slab.

The rest of this paper is organized as follows. Section II gives the deformation model of the rolling process. Section III establishes the DT model. Section IV designs the wide adjustment controller by the SSC method. Section V simulates the numerical example. Section VI gives the summary and looks forward to the future work.

II. DEFORMATION MODEL ESTABLISHMENT OF ROLLING PROCESS

A. DESCRIPTION OF ROLLING PROCESS

Currently, the main study in the control of rolling systems include the development of accurate mathematical models (describe the dynamics of the rolling process, including the material deformation, friction, and other factors affecting the system's behavior), feedback control techniques (measure relevant system variables, such as roll force, thickness, or temperature, and use this information to adjust the control inputs in real time), adaptive control methods

(continuously monitor the system's behavior and adjust the control parameters accordingly to maintain optimal performance), model predictive control (utilize a mathematical model of the rolling system to predict its future behavior), neural network control approaches (learn the complex mapping between system inputs and outputs, allowing for adaptive and nonlinear control), and real-time monitoring and visualization tools (monitor critical variables, detect anomalies, and make informed decisions to optimize the control actions). These advancements have led to improved performance, quality, and efficiency in rolling processes, benefiting industries that rely on metal manufacturing.

In a general hot rolling production line, the rough rolling unit consists of a set of reversing rolling mills E1 and R1, two pyrometers and a width gauge. The rolling line layout is shown in Fig. 1. The rough rolling width control target is determined according to the finished strip width, finish rolling allowance and finish rolling width. And then the rolling initial setting calculation is carried out in combination with the relevant information of incoming materials. After each pass of rolling is completed, the rolling setting value of the subsequent pass is adjusted according to the actual width data measured by the width gauge to ensure that the rough rolling exit width can hit the target.

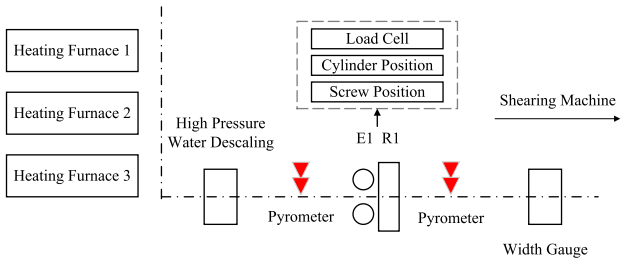

FIGURE 1. Hot rolling production line.

The general process starts with the feeding of the raw slab into the roughing mill, where it undergoes compression and length increase in the E1 mill. Next, it enters the R1 mill for shape adjustment and surface quality treatment. And the load cell, the cylinder position and the screw position are deployed on the rolls to measure the roll gap and rolling force, respectively. Throughout the process, the pyrometer monitor the slab temperature, while the width gauge precisely measures the slab's width.

It can be seen from the above rolling process that the key factor affecting the accuracy of the rolling process is the determination of the rough rolling width and thickness, that is, the selection of the roll gap. Regardless of thickness setting or width setting, it is first necessary to determine the thickness and width distribution of each pass, that is, the reduction amount of each pass of rough rolling is distributed reasonably, then the slab with a thickness of H can be rolled out of a strip with a thickness of H_c through multiple passes of rough rolling. On the one hand, the choice of H_c should consider that the roughing mill can roll the slab from H to H_c with odd or even passes. On the other hand, it should also be determined according to the thickness of the finished product to be rolled and the load of the finishing rolling unit.

When H_c is determined, the task is to determine the number of passes. For a single-stand reversing roughing mill, the average reduction $\triangle H_m$ can be calculated based on [29].

$$\triangle H_m = \frac{1}{R}\left(\frac{1.9 \times 971N}{n_m P_m}\right)^2 \tag{1}$$

where n_m is the average speed of rolls in each pass, P_m is the average rolling force of each pass, N is the motor power and R is the roll radius. Then, the number of passes is

$$RN = \frac{H - H_c}{\Delta H_m} \tag{2}$$

And the reduction amount of the jth pass is

$$\begin{aligned} \Delta H_j &= \delta_j \sum_{\varsigma=1}^{RN} \Delta H_\varsigma \\ \sum_{\varsigma=1}^{RN} \Delta H_\varsigma &= H - H_c \end{aligned} \tag{3}$$

where δ_j is the distribution coefficient of reduction in the jth pass.

For the width, the slab width B and the rough rolling exit width B_c also should be determined first. B_c is slightly wider than the finished product width B_n to prevent the looper and coiler from narrowing the bandwidth.

$$B_c = B_n + \Delta \tag{4}$$

where $\Delta \in [5mm, 10mm]$. And the width reduction of each vertical roller is

$$\begin{aligned} \Delta B_{Eij} &= \Delta B_{E\Sigma} \xi_{ij} \\ \Delta B_{E\Sigma} &= (1.015B - B_c) + \sum DB_{Rij} \end{aligned} \tag{5}$$

where ξ_{ij} is the width reduction distribution coefficient, DB_{Rij} is the spread amount of the ith rack and the jth pass, $\Delta B_{E\Sigma}$ is the total width reduction and ΔB_{Eij} is the width reduction of the ith vertical roller in the jth pass.

B. RIGID-VISCOPLASTIC FE METHOD

At a certain moment of quasi-static deformation, the deformed body is in equilibrium. Let the volume of the deformed body be v and the surface be S. Stress boundary conditions are given on the force boundary S_F, and the displacement boundary conditions are given on the velocity boundary S_v. Then the real solution of the rigid-viscoplastic FE makes the following functional take the extremum [30], [31].

$$\Pi = \int_v \bar{\sigma}\dot{\bar{\varepsilon}} dv - \int_{S_F} F_i u_i dS \tag{6}$$

where $\bar{\sigma}$ is the equivalent stress, $\dot{\bar{\varepsilon}}$ is the equivalent strain rate, F_i is the given surface force on the force boundary S_F,

u_i is the given velocity on the velocity boundary S_v. Introducing the volume incompressibility condition into Eq. (6), the first-order variational expression is obtained as

$$\Pi = \int_v \bar{\sigma}\dot{\bar{\varepsilon}}dv + \frac{\alpha}{2}\int_v (\dot{\varepsilon}_v)^2 dv - \int_{S_F} F_i u_i dS \tag{7}$$

where α is the penalty factor, $\dot{\varepsilon}_v$ is the equivalent volumetric strain rate. Using an eight-node hexahedron isoparametric element to discretize the deformation body, then we get the velocity component at any point in the element $\{u\} = [N]\{u\}^e$, where $[N]$ is the shape function matrix, $\{u\}^e$ is the unit node velocity vector. Therefore, the strain rate component at any point in the element can be obtained as $\left\{\dot{\bar{\varepsilon}}\right\} = [L][N]\{u\}^e = [B]\{u\}^e$, where $[L]$ is the differential operator matrix, $[B]$ is the element strain rate matrix. Finally, the deformable body is divided into m units and n nodes, and the velocity field is obtained according to techniques such as variational principle, iterative algorithm and Taylor series expansion.

$$\left\{u^e\right\}_n = \left\{u^e\right\}_{n-1} + \left\{\Delta u^e\right\} \tag{8}$$

where $\{\Delta u^e\}$ satisfies

$$\begin{aligned}&\sum_{e=1}^{m}\left([P]_{n-1} + [M]\right)\left\{\Delta u^e\right\} \\ &\quad = \sum_{e=1}^{m}\left(\{f\} - [H]_{n-1} - [M]\left\{u^e\right\}_{n-1}\right)\end{aligned} \tag{9}$$

where

$$\begin{aligned}[P]_{n-1} &= \frac{2}{3}\bar{\sigma}\int_{S_v^e}\frac{1}{\dot{\bar{\varepsilon}}_{n-1}}\left[[K] - \frac{2}{3}\frac{1}{\dot{\bar{\varepsilon}}_{n-1}}[K]\left\{u^e\right\}_{n-1}\right. \\ &\qquad \left.\left\{u^e\right\}_{n-1}^T[K]\right]dv \\ [M] &= \alpha\int_{S_v^e}[B]^T[C][C]^T[B]\,dv,\ \{f\} = \int_{S_F}[N]^T\{F\}\,dS \\ [H]_{n-1} &= \frac{2}{3}\bar{\sigma}\int_{S_v^e}\frac{1}{\dot{\bar{\varepsilon}}_{n-1}}[K]\left\{u^e\right\}_{n-1}dv,\ [K] = [B]^T[B] \\ [C] &= \begin{bmatrix}1 & 1 & 1 & 1 & 0 & 0 & 0 & 0\end{bmatrix}^T\end{aligned} \tag{10}$$

Finally, an approximate real solution that satisfies the accuracy requirements can be obtained.

C. SOLVING THE DEFORMATION MODEL OF ROLLING PROCESS

Since the rolled piece is in a high-temperature state during the rough rolling process, the rolled piece is treated as a rigid plastic body material and the roll is regarded as a non-deformable rigid body. Therefore, the rigid-viscoplastic FE method (6), (7) can be used to establish the deformation model of the width adjustment rolling process.

It is worth noting that the general deformation law of the slab width adjustment rolling process has been summarized through long-term field rolling experiments. The slab shape after rolling can be described by six parameters: head loss, head length, tail loss, tail length, tail inflection point loss and tail inflection point loss length. Then, according to the literature [32], [33], these parameters are determined by the slab geometry, material, width reduction, vertical roll diameter and environmental factors. Therefore, the slab model is established and the shape parameters are calculated using the rigid-viscosity-plastic FE method. The simulation calculation algorithm is shown in Fig. 2, and the specific process is as follows:

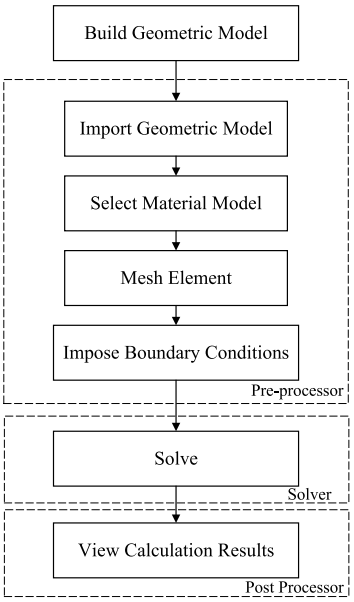

FIGURE 2. DEFORM-3D simulation calculation process.

1. Use computer-aided design (CAD) software to construct the geometric model of continuous casting slab width adjustment rolling simulation. The geometric model of the roll and the rolled piece is mainly determined by the vertical roll, the horizontal roll and the slab. The first stand vertical roll of the roughing mill generally has two types–flat vertical roll and grooved vertical roll. The horizontal roll is all in the form of the flat roll body, and the slab raw materials are reasonably selected.

2. Use DEFORM-3D software to solve Eq. (7), which consists of three parts: pre-processor, solver and post processor. The tasks of the pre-processor include importing the geometric model, selecting the material model of the rolled piece, meshing the geometric model and applying boundary loads. The material model is described by the rate-dependent plastic model, and the four-node tetrahedron isoparametric element is used to divide the grid of the slab. The selection of boundary conditions is based on the symmetry of the slab shape and the boundary conditions. Only 1/4 of the slab is taken for research, and symmetrical constraints are imposed on the two symmetrical planes in the center. The tasks of the solver and post processor are to solve the algorithm and view the calculation results, respectively.

III. SLAB SHAPE OF HEAD AND TAIL DT REALIZATION ARCHITECTURE

The method of using the rigid-viscoplastic FE method to obtain the head and tail shape of the continuous casting slab after width adjustment rolling requires a large amount of calculation and takes a long time, which cannot satisfy the requirement of actual production online control. Therefore, it is necessary to establish an online calculation model for the slab shape parameters of the head and tail for real-time control. In this section, the MPL is considered to calculate the slab shape parameters of the head and tail online, and the corresponding DT model is obtained.

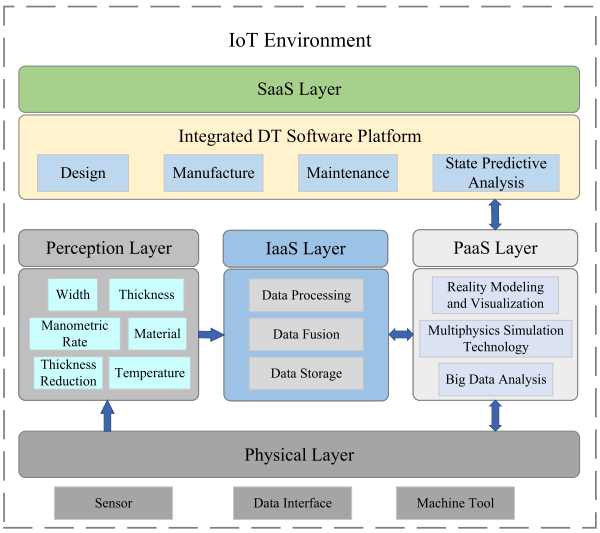

FIGURE 3. DT implementation framework.

The DT-oriented slab shape of head and tail online prediction system creates a virtual scene based on the real scene, connects the two scenes through the sensing and data interaction interface to form a closed-loop data exchange channel, and realizes virtual-real mapping and two-way iterative optimization between physical equipment and digital space. Realizing the digital twin of the hot rolling process requires the Internet of Things (IoT) platform as a carrier, and the digital twin realization architecture is shown in Fig. 3, which mainly includes physical layer, edge layer, Infrastructure-as-a-Service (IaaS) layer, Platform-as-a-Service (PaaS) layer, and Software-as-a-Service (SaaS) layer.

The physical layer serves as the foundation of the digital twin implementation and includes the actual physical devices and sensors. In the context of hot rolling, the physical layer encompasses equipment such as rolling mills, sensors, and cameras that are used for sensing and capturing real-time data. The edge layer is situated on-site or in close proximity to the site, acting as a bridge between the physical layer and the cloud platform. It possesses computational and storage capabilities for processing and analyzing real-time data. In the case of hot rolling, the edge layer can execute real-time data processing and predictive models, providing real-time decision support and control instructions. The IaaS layer provides the foundational infrastructure resources, including computing, storage, and networking. Within the digital twin implementation, the IaaS layer furnishes the necessary computing and storage capabilities to support tasks such as data processing, model training, and inference. The PaaS layer delivers the software and development tools required for the digital twin platform. It supports the development, deployment, and management of digital twin applications, encompassing functionalities such as data management, model management, and visualization. In the context of hot rolling, the PaaS layer can provide real-time data visualization, model training, and optimization algorithm management. The SaaS layer offers cloud-based applications and services directly accessible to users. Within the digital twin implementation, the SaaS layer provides the online prediction system and analytical tools specific to the hot rolling process. This empowers users to monitor and optimize the hot rolling process, enhancing production efficiency and product quality. Together, these layers form the architecture of a digital twin implementation. By leveraging physical devices, edge computing, cloud platforms, and application software, it enables data exchange and iterative optimization between the real and virtual scenes. This integration enhances the visualization, intelligence, and control capabilities of the hot rolling process.

The DT model is built as a three tuple:

$$DT = \{P, V, C\} \tag{11}$$

where P represents the actual data collection based on sensors in the physical space, V represents the DT of physical entities and intelligent entities constructed based on simulation technology in virtual space, C represents the connection method of the two spaces, which solves the problem of real-time data transmission and fast update.

A. PHYSICAL ENTITY P

The physical entity model P is composed of various functional subsystems and sensing devices to realize the perception and collection of massive data on the status of sources, networks, loads and storage links in the real world. In this paper, the measurement data are obtained according to the rigid-viscoplastic FE method model.

B. VIRTUAL MODEL V

The virtual model V is the mapping of the physical entity, which realizes the mirror copy of the real world in the virtual space. That is, physical entities are modeled as virtual mechanisms. The model has attributes such as processing action behavior, signal transmission and control, and has the ability to reproduce the production activities of the physical workshop.

MLP can enable the idea of mapping from data to models, the principle is shown in Fig. 4. Take the FE simulation results as the original sample data set. In order to avoid and reduce the data range of the initial variable, it is necessary to perform feature scaling on the data. And the dataset is divided into

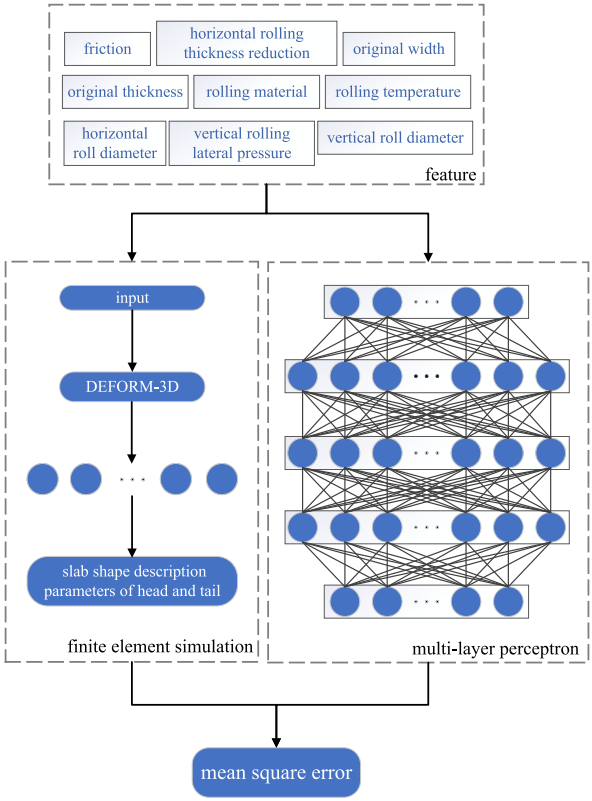

FIGURE 4. MLP network structure and principles of training with FE data.

training set and test set. The training sample features are selected as vertical rolling width reduction ΔB, horizontal rolling thickness reduction ΔH, slab original width B, slab original thickness H, vertical roll diameter R_E, horizontal roll diameter R_H, rolling material M, rolling temperature T and friction f. The prediction output is the slab shape description parameters of the head and tail, including loss of head width ΔW_H, loss length of head width ΔL_H, loss of tail width ΔW_T, loss length of tail width ΔL_T, loss of tail inflection point ΔW_{CT} and loss length of tail inflection point ΔL_{CT}.

Based on the number of features and the number of prediction parameters, the network structure of MLP is defined, that is, the number of layers in the hidden layer, the number of nodes in the input layer, each hidden layer and the output layer are determined, respectively. On the basis of creating the model, random initialization of weights and biases is performed to initialize the model. Mean squared error MSE is selected as the loss function, the equation is as follows:

$$MSE = \frac{1}{n} \cdot \sum_{k=1}^{n} \left\| Y_k - Y'_k \right\|^2 \tag{12}$$

where $Y_k = \{\Delta W_H, \Delta L_H, \Delta W_T, \Delta L_T, \Delta W_{CT}, \Delta L_{CT}\}$ is the true value, and Y'_k is the corresponding predicted value. MSE measures the closeness between the real value and the predicted value, and the smaller the value, the smaller the error of the predicted value.

Then, the gradient is calculated by the backpropagation algorithm, and the optimizer is used to update the weights and biases of the model, the equation is as follows:

$$\begin{cases} w_i^{(k+1)} = w_i^{(k)} - g_i^{(k)} \\ g_i^{(k)} = \dfrac{\eta \hat{v}_i^{(k)}}{\sqrt{\hat{s}_i^{(k)}} + \theta} \end{cases} \tag{13}$$

where $g_i^{(k)}$ is the distance that the ith parameter of MLP descends along the gradient direction at the kth iteration, $v_i^{(k)}$ and $s_i^{(k)}$ are the exponentially decaying averaging of historical gradient square and the exponentially decaying averaging of historical gradient, respectively. $\hat{v}_i^{(k)}$ and $\hat{s}_i^{(k)}$ are the bias corrections of $v_i^{(k)}$ and $s_i^{(k)}$, respectively. And

$$\begin{cases} \hat{v}_i^{(k)} = \dfrac{v_i^{(k)}}{1-\sigma_1} \\ \hat{s}_i^{(k)} = \dfrac{s_i^{(k)}}{1-\sigma_2} \\ v_i^{(k+1)} = \sigma_1 v_i^{(k)} + (1-\sigma_1) \dfrac{\partial MSE}{\partial w_i} \left(w^{(k)} \right) \\ s_i^{(k+1)} = \sigma_2 s_i^{(k)} + (1-\sigma_2) \left(\dfrac{\partial MSE}{\partial w_i} \left(w^{(k)} \right) \right)^2 \end{cases} \tag{14}$$

where σ_1 and σ_2 are learning rate hyperparameters, and the process is repeated until the stopping condition is reached.

C. CONNECTION C

C is the connection between the physical entity and the data platform, the connection between the physical entity and the virtual space, the connection between the physical entity and the intelligent entity, the connection between the data platform and the virtual space, the connection between the data platform and the intelligent entity and the connection between the virtual space and the intelligent entity. It is also a network platform for building DT systems.

IV. SHORT STROKE CONTROL

In the actual production process, the short stroke control (SSC) technology adjusts the vertical roll gap during vertical rolling to change the shape of head and tail and dog bone distribution of slab. Therefore, it offsets the width change during subsequent horizontal rolling, and obtains a qualified slab whose width fluctuation is controlled within a certain range. In the case of other conditions being the same, the change in the thickness reduction during horizontal rolling will not only cause the change in the width loss at the head and tail, but also change the slab shape of the head and tail, especially the tail. Then, it is necessary to determine the form of the short stroke curve according to the slab shape after horizontal rolling. Generally speaking, the FE algorithm can obtain short stroke curve parameters. However, the algorithm has a large amount of calculation, and it is difficult to be extended to different production lines

for real-time calculation. Therefore, Therefore, the MPL is considered to predict the short stroke curve online and realize the synchronous width adjustment of SSC technology.

In general, through the width reduction of the vertical roll and the thickness reduction of the horizontal roll, the width loss phenomenon will occur at the slab head and tail. The slab shape of the head is the loss-of-width type, and the shape of the tail is the loss-of-width type, the fishtail type and the widening type. The three-stage SSC form is adopted, as shown in Fig. 5, where the head control segment is composed of a slash segment, the control parameters are BH1 and LH1. The tail control segment is composed of two consecutive slash segments, the control parameters are BT1, BT2, LT1 and LT2. When the tail shape is widened or lost, BT1=BT2 and LT1=LT2, the tail of the short stroke curve degenerates into a straight line.

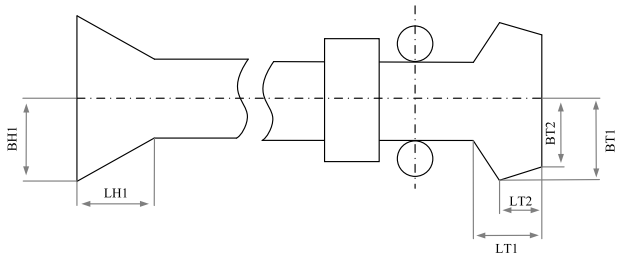

FIGURE 5. Three-stage SSC and control parameters.

Based on the DT model (11), the SSC parameter calculation model is designed, and the control length equation is as follows:

$$\begin{aligned} LH1 &= \omega_{LH} \cdot \Delta L_H \cdot (1-\varepsilon_H)^{\alpha} \\ LT1 &= \omega_{LT1} \cdot \Delta L_T \cdot (1-\varepsilon_H)^{\beta} \\ LT2 &= \omega_{LT2} \cdot \Delta L_{CT} \cdot (1-\varepsilon_H)^{\beta} \end{aligned} \tag{15}$$

where α is the head extension coefficient, β is the tail extension coefficient, ε_H is the thickness reduction, ω_{LH}, ω_{LT1} and ω_{LT2} are the adaptive coefficient of SSC length.

Meanwhile, the control width equation is as follows:

$$\begin{aligned} BH1 &= ZAS + \omega_{BH} \cdot \Delta W_H \cdot (1-\varepsilon_E)^{1.1}(1-\varepsilon_H)^{0.9} \\ BT1 &= ZAS + \omega_{BT1} \cdot \Delta W_{CT} \cdot (1-\varepsilon_E)^{1.2}(1-\varepsilon_H)^{0.83} \\ BT2 &= ZAS + \omega_{BT2} \cdot \Delta W_T \cdot (1-\varepsilon_E)^{1.2}(1-\varepsilon_H)^{0.83} \end{aligned} \tag{16}$$

where zero adjustment system (ZAS) is the static opening of vertical rolling mill, ε_E is the width reduction rate during vertical rolling, ω_{BH}, ω_{BT1} and ω_{BT2} are the self-adaptation of SSC width coefficient.

In summary, the deformation model of the widening rolling process established by the rigid viscoplastic FE method is used to obtain the measured data. Based on DT model (11), combined with Eqs. (15) and (16), the deformation curve is obtained and the prediction result is transferred to the SSC system to get the automatic control system of head and tail shape of continuous casting slab rough rolling. Ultimately, the width control over the full length of the slab is achieved.

V. NUMERICAL SIMULATION

In this section, the slab parameters first set based on the actual working environment of the wide and thick plate factory of a steel plate division, as shown in Tab. 1.

TABLE 1. The slab parameters.

parameter	value
vertical rolling width reduction	50, 60, 70, 80, 90, 100 mm
horizontal rolling thickness reduction	10, 20, 30, 40, 70 mm
width	900, 1000, 1200, 1300, 1400, 1500, 1600, 1700, 1900 mm
thickness	200, 230, 250 mm
vertical roll diameter	1050 mm
horizontal roll diameter	1250 mm
rolling material	1045 steel, 4340 steel
rolling temperature	$1100°C$
friction coefficient	0.5

First, based on Rigid-viscoplastic FE method, DEFORM-3D software is used to get 870 sample sets, and the slab shape of the head and tail after vertical rolling are shown in Figs. 6 and 7.

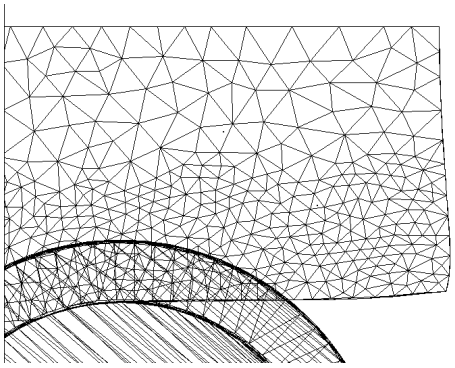

FIGURE 6. The slab shape of head after vertical rolling.

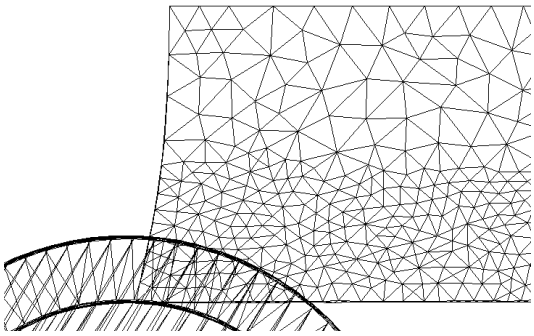

FIGURE 7. The slab shape of tail after vertical rolling.

Then, the results of FE simulation calculations are used as training samples, a total of 600 groups, to train the DT model for the slab shape of the head and tail parameter prediction,

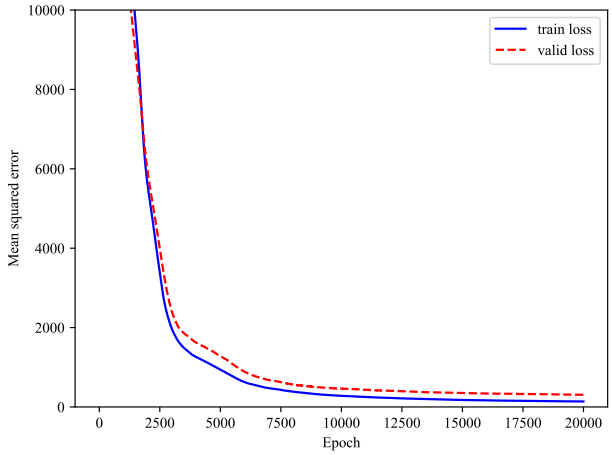

FIGURE 8. The value of the loss function.

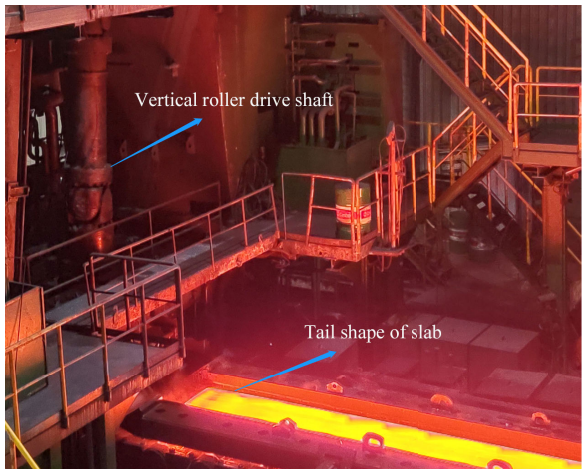

FIGURE 9. A rough rolling mill.

TABLE 2. Curve control parameters.

parameter	value
BH1	531
LH1	605
BT1	508
BT2	505
LT1	558
LT2	249

and 270 groups are used as model test sets. The loss function (12) are shown in Fig. 8. After iterating for 20000 steps, the results converge.

In the algorithm implementation process, we deploy a post-rolling online width gauge to achieve real-time monitoring of material width variations. The post-rolling online width gauge can not only measure the head and tail shape and width of the rolled product, but also utilize the actual measurement values to reflect and correct errors in the control model. By accumulating production data and continuously learning, this approach ensures the effectiveness of the control system.

Finally, we test the automatic control system of head and tail shape of continuous casting slab rough rolling with a slab with a geometric size of 3500mm×1600mm×250mm. Taking a steel factory conducts tests, as shown in Fig. 9,

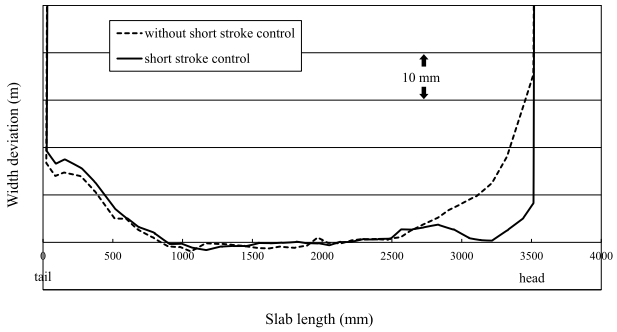

FIGURE 10. Short stroke curves implementation effect.

combined with DT model (11), we obtained the SSC parameters (Tab. 2) and short stroke curves implementation effect (Fig. 10).

VI. CONCLUSION

In this paper, we propose a novel approach for online width adjustment control of continuous casting slabs based on the digital twin framework. Our methodology involves the use of a deformation model that takes into account the material mechanical properties, geometric model, and boundary conditions of the continuous casting slab rolling process using the rigid-viscoplastic finite element method. By analyzing the shape parameters of the head and tail of the rolled piece, we are able to design features that capture the deformation characteristics of the slab. Using these features and a multilayer perceptron, we develops a digital twin model that can accurately predict the loss-width curve at the head and tail of the slab in real-time. Our proposed method enables the synchronous correction of the roll gap of the vertical roll mill to achieve the desired width adjustment of the continuous casting slab, thereby reducing production costs. In the simulation, we use the post-rolling online width gauge to measure the head and tail shape and width of the rolled product, and then the error is corrected by accumulating production data and continuously learning the model. The result shows the accuracy and effectiveness of the proposed method.

In future work, we plan to expand the scope of our approach to include other types of deformation phenomena that may occur during slab rolling, such as edge cracks and surface defects. We also aim to investigate the impact of various process parameters, such as casting speed and cooling rate, on the deformation behavior of continuous casting slabs.

REFERENCES

[1] X. Zhang, L. Ma, K. Peng, and C. Zhang, "A quality-related distributed fault detection method for large-scale sequential processes," *Control Eng. Pract.*, vol. 127, Oct. 2022, Art. no. 105308.

[2] F. Peng, L. Zheng, Y. Peng, C. Fang, and X. Meng, "Digital twin for rolling bearings: A review of current simulation and PHM techniques," *Measurement*, vol. 201, Sep. 2022, Art. no. 111728.

[3] M. J. Neuer, M. Loos, F. Marchiori, V. Colla, S. Dettori, J. Ordieres, and A. Wolff, "From controlling single processes to the complex automation of process chains by artificially intelligent control systems: The control in steel project," *IFAC-PapersOnLine*, vol. 55, no. 40, pp. 295–300, 2022.

[4] N. Tazoe, "Prevention of fish tail during intensive edging in hot roughing mill line," *IHI Eng. Rev.*, vol. 14, pp. 42–47, Jan. 1981.

[5] M. Matsuzaki, S. Kanari, Y. Ogawa, and Y. Nakazato, "A new method of slab rolling for prevention of growth of crops," *Tetsu-Hagane*, vol. 67, no. 15, pp. 2350–2355, 1981.

[6] T. Shikimori, S. Muto, and O. Yamaguchi, "Development of automatic rolling scheduling system for synchronized operation of casting and hot rolling," *IFAC-PapersOnLine*, vol. 49, no. 20, pp. 250–255, 2016.

[7] X.-Z. Du, Q. Yang, C. Lu, A.-L. Wang, and T. A. Kiet, "Optimization of short stroke control preset for automatic width control of hot rolling mill," *J. Iron Steel Res. Int.*, vol. 17, no. 6, pp. 16–20, Jun. 2010.

[8] Y.-M. Liu, D.-H. Zhang, J. Sun, and D.-W. Zhao, "Theoretical study of rolling force during width control in edge rolling," in *Proc. Chin. Control Decis. Conf. (CCDC)*, May 2016, pp. 1176–1179.

[9] E. Moya-Lasheras, E. Ramirez-Laboreo, and C. Sagues, "Probability-based optimal control design for soft landing of short-stroke actuators," *IEEE Trans. Control Syst. Technol.*, vol. 28, no. 5, pp. 1956–1963, Sep. 2020.

[10] T. Shubin, L. Long, and L. Jianchang, "Research on the gap setting model of short stroke control system in hot edge rolling," in *Proc. Chin. Control Decis. Conf. (CCDC)*, May 2011, pp. 4126–4128.

[11] E. Moya-Lasheras and C. Sagues, "Run-to-run control with Bayesian optimization for soft landing of short-stroke reluctance actuators," *IEEE/ASME Trans. Mechatronics*, vol. 25, no. 6, pp. 2645–2656, Dec. 2020.

[12] S. Xiong, X. Zhu, and C. Wang, "Experiments on edge rolling with flat rolls in roughing trains of hot strip mills," *Steel Rolling*, vol. 10, pp. 2–5, Jan. 1996.

[13] L. Liu, J. Zhang, C. Song, K. He, A. A. Saputra, and W. Gao, "Automatic scaled boundary finite element method for three-dimensional elastoplastic analysis," *Int. J. Mech. Sci.*, vol. 171, Apr. 2020, Art. no. 105374.

[14] P. Jian-Yi, Z. Zhao-Yao, W. Yao, L. Liang, and H. Ke-Jing, "Numerical simulation applications of aluminum extrusion engineering based on rigid-plastic finite element method," in *Proc. Int. Conf. Mechanic Autom. Control Eng.*, Jun. 2010, pp. 334–338.

[15] X. Pei, J. Du, and G. Chen, "Accelerated nonlinear finite element method for analysis of isotropic hyperelastic materials nonlinear deformations," *Appl. Math. Model.*, vol. 120, pp. 513–534, Aug. 2023.

[16] M. S. Joun, J. H. Chung, and R. Shivpuri, "An axisymmetric forging approach to preform design in ring rolling using a rigid-viscoplastic finite element method," *Int. J. Mach. Tools Manuf.*, vol. 38, nos. 10–11, pp. 1183–1191, Oct. 1998.

[17] Y. Tan, Y. Chi, Y. Huang, and T. Yao, "Three-dimensional rigid-viscoplastic finite element simulation of milling process," in *Proc. Int. Conf. Mechanic Autom. Control Eng.*, Jun. 2010, pp. 211–215.

[18] P. R. P. Carvalho, H. B. Coda, and R. A. K. Sanches, "A large strain thermodynamically-based viscoelastic-viscoplastic model with application to finite element analysis of polytetrafluoroethylene (PTFE)," *Eur. J. Mech.-A/Solids*, vol. 97, Jan. 2023, Art. no. 104850.

[19] Z. Liang, J. Li, X. Zhang, and Q. Kan, "A viscoelastic-viscoplastic constitutive model and its finite element implementation of amorphous polymers," *Polym. Test.*, vol. 117, Jan. 2023, Art. no. 107831.

[20] W. Jia, W. Wang, and Z. Zhang, "From simple digital twin to complex digital twin—Part II: Multi-scenario applications of digital twin shop floor," *Adv. Eng. Informat.*, vol. 56, Apr. 2023, Art. no. 101915.

[21] P. Bellavista, N. Bicocchi, M. Fogli, C. Giannelli, M. Mamei, and M. Picone, "Requirements and design patterns for adaptive, autonomous, and context-aware digital twins in Industry 4.0 digital factories," *Comput. Ind.*, vol. 149, Aug. 2023, Art. no. 103918.

[22] J. Guo, R. Jia, R. Su, and Y. Zhao, "Identification of FIR systems with binary-valued observations against data tampering attacks," *IEEE Trans. Syst., Man, Cybern., Syst.*, vol. 53, no. 9, pp. 5861–5873, Sep. 2023, doi: 10.1109/TSMC.2023.3276352.

[23] J. Guo and J.-D. Diao, "Prediction-based event-triggered identification of quantized input FIR systems with quantized output observations," *Sci. China Inf. Sci.*, vol. 63, no. 1, pp. 1–12, Jan. 2020.

[24] J. Zhao, X. Xiong, and Y. Chen, "Design and application of a network planning system based on digital twin network," *IEEE J. Radio Freq. Identificat.*, vol. 6, pp. 900–904, 2022.

[25] Y. Zhou, J. Tang, X. Yin, W. Xie, L. Jia, G. Xiong, and H. Zhang, "Digital twins visualization of large electromechanical equipment," *IEEE J. Radio Freq. Identificat.*, vol. 6, pp. 993–997, Oct. 2022.

[26] T. Li, H. Shi, X. Bai, and K. Zhang, "A digital twin model of life-cycle rolling bearing with multiscale fault evolution combined with different scale local fault extension mechanism," *IEEE Trans. Instrum. Meas.*, vol. 72, pp. 1–11, 2023.

[27] F. Xiang, S. Zhou, Y. Zuo, and F. Tao, "Digital twin driven end-face defect control method for hot-rolled coil with cloud-edge collaboration," *IEEE Trans. Ind. Informat.*, vol. 19, no. 2, pp. 1674–1682, Feb. 2023.

[28] M. Lippi, M. Martinelli, M. Picone, and F. Zambonelli, "Enabling causality learning in smart factories with hierarchical digital twins," *Comput. Ind.*, vol. 148, Jun. 2023, Art. no. 103892.

[29] Y. Sun, *Daigang Relianzha de Moxing yu Kongzhi*. Beijing, China: Metallurgical Industry Press, 2007.

[30] O. C. Zienkiewicz and P. N. Godbole, "A penalty function approach to problems of plastic flow of metals with large surface deformations," *J. Strain Anal.*, vol. 10, no. 3, pp. 180–183, Jul. 1975.

[31] J. J. Park and S. Kobayashi, "Three-dimensional finite element analysis of block compression," *Int. J. Mech. Sci.*, vol. 26, no. 3, pp. 165–176, Jan. 1984.

[32] S. Xiong, X. Liu, G. Wang, Q. Zhang, L. Han, X. Zhao, and T. Chen, "Slab width reduction technology in roughing trains of hot strip mills and methods for improvement of crop loss," *Iron Steel*, vol. 29, no. 12, pp. 75–78, 1994.

[33] S. Xiong, X. Zhu, X. Liu, G. Wang, and Q. Zhang, "Deformation behaviors of materials during width reduction by flat edger roll in roughing trains of hot strip mill," *Res. Iron Steel*, vol. 3, pp. 17–20&24, Jan. 1996.

CHAOQUN SONG is currently pursuing the degree in material forming and control engineering with the School of Metallurgical Engineering, Anhui University of Technology, under the supervision of Professor Xiaohui Shen. He has been involved in the topic of "Research on continuous casting billet rolling with adjustable width," responsible for finite element analysis, data sorting, machine learning modeling, and other work. His research interests include metal processing and forming technology, finite element analysis, and machine learning.

XIAOHUI SHEN received the bachelor's degree majoring in pressure processing from the East China Institute of Metallurgy, in 1997, the master's degree in material processing engineering from the University of Science and Technology Beijing, in 2002, and the Ph.D. degree in material processing engineering from the Nanjing University of Aeronautics and Astronautics, in 2013. Since July 1997, he has been teaching with the Department of Material Forming, Anhui University of Technology, engaged in the teaching and research of plastic forming theory and technology. He has published more than 30 academic articles and authorized five invention patents. His research interests include plastic forming theory and process, and material processing simulation.

JUNCHAO XIA received the B.E. degree in engineering management from Sanjiang University, and the M.E. degree in materials science and engineering from the Anhui University of Technology, in 2023. From 2020 to 2023, he was a Research Assistant to Professor Xiaohui Shen. He has published two articles. He has participated in a number of research topics, such as "Development of high precision flexible rolling technology for high-quality bars," and "Research on continuous casting billet rolling with adjustable width." His research interests include finite element analysis and numerical simulation.